

Propagation of mechanical waves in a one-dimensional nonlinear disordered lattice

O. Richoux, C. Depollier, and J. Hardy

Laboratoire d'Acoustique de l'Université du Maine, UMR-CNRS 6613, Av. Olivier Messiaen, 72085 Le Mans cedex 9, France

(Received 30 April 2004; revised manuscript received 13 October 2005; published 17 February 2006)

The propagation of transverse waves along a string loaded by N masses, each of them being fixed to a spring with a quadratic nonlinearity, is studied. After presenting the nonlinear model and stating the equation of propagation into a lattice with discrete nonlinearities and disorder, we propose a perturbation approach to wave propagation in a nonlinear lattice using the Green's function formalism. We show how the nonlinearity acts on the propagation into a disordered lattice. In the low-frequency approximation, an analytical expression of the boundary between the propagative regime and the evanescent one is found. Numerical results are compared to the analytical results and phase diagrams are proposed in the ordered and disordered cases. A behavior of the transmission coefficient is found, on an empirical basis, as a function of the length of the lattice and the localization length in the nonlinear case. Finally, a dynamic approach is developed and the ordered and disordered cases are addressed. This method is based on a finite difference equation and allows the construction of the Poincaré section describing the propagation of the wave into the lattice. This approach distinguishes between the properties of propagation in the lattice in a propagative regime and in an evanescent one.

DOI: [10.1103/PhysRevE.73.026611](https://doi.org/10.1103/PhysRevE.73.026611)

PACS number(s): 46.40.-f, 82.40.Bj, 05.45.-a, 42.65.Wi

I. INTRODUCTION

Anderson localization phenomena have been studied mainly in linear random media [1,2]. Up to now, it has been clearly established that the disorder precludes the presence of long-range propagation.

However, two scenarios have been put forward to suppress localization and to allow the propagation of waves: correlation in disorder [3–5] and nonlinearity [6–17]. For electronic motion, it was proven that the presence of an electric field can break the localization process [18,19]. Although the former has been shown to improve transport properties, it is beginning to seem that nonlinear waves may be strong enough to propagate even in the presence of disorder.

Indeed, up to now, very little is known on the interplay of nonlinearity and the classical wave localization (for a review see [20]). Beloshapkin *et al.* [21] have suggested a closed relation between the disorder in particle chains and the dynamic problem of transition to chaos. Recently, Sayar *et al.* [9] examined the effects of nonlinearity on the localization behavior observed in one-dimensional linear and nearly periodic structures. In particular, they show that nonlinear neighbor interactions delocalize the modes corresponding to low frequencies. Furthermore, Cai *et al.* [22] studied the localized modes of periodic systems having nonlinear disorders. On the basis of exact solutions for a set of nonlinear algebraic solutions, they concluded that the localized modes exist for any amount of the ratio between the linear coupling stiffness and the nonlinear disorder parameter.

In parallel, the theory of the wave transmission in nonlinear ordered lattices is now well known (for a review see [23]). A great number of experimental studies have been done in optics (light scattering experiments) or quantum physics but, with classical waves, the works are very few. We can cite McKenna and co-workers [10,11] which examined experimentally the propagation of transversal waves in a wire loaded by masses and showed qualitatively the influence of the nonlinearity due to the wire on the Anderson localization.

In this context, it is the purpose of this paper to examine the interplay between the effects of disorder and nonlinearity on the propagation of classical waves by means of an analytical model and numerical simulations, in the case of a quasi-one-dimensional string loaded by N mass-spring systems.

We analyze this nonlinear problem by looking at the effect on the wave propagation of nonlinear terms in the wave equation in the model. These nonlinear terms model the nonlinear response of springs at each node of the lattice. The question is: what is the influence of discrete nonlinearities on propagation in a disordered lattice?

In the first section, the wave propagation in the lattice with discrete nonlinearities is formulated through recurrence relations and wave “transfer” operators. The weak nonlinearity case is analytically solved with the help of a perturbation method and an analytical result is found for the low-frequency case.

The last part presents another way to examine the interplay between disorder and nonlinearity: an area-preserving nonlinear mapping is used to describe this kind of propagation. Finally, the main results are summarized in the conclusion.

II. PRESENTATION OF THE NONLINEAR MODEL

In this paper, we focused on the transverse vibrations $y(x,t)$ of an infinite string loaded between $x=0$ and $x=L$ by N spring-mass systems acting as resonators, constituting a lattice (see Fig. 1). The n th cell characterized by the mass M_n and the stiffness constant of the spring k_n is located at x_n and the lattice spacing is defined by $d_n=x_{n+1}-x_n$. (see Fig. 2).

In the remainder of the paper, two cases are investigated. In the first one, all the physical attributes of the lattice are identical ($M_n=M$, $k_n=k$ and $x_{n+1}-x_n=d$, $\forall n$). In such circumstances, the system constitutes a periodic lattice. In the second case, the masses M_n , the stiffnesses k_n of the springs,

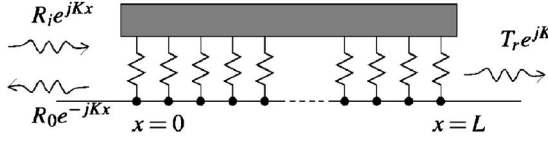


FIG. 1. Picture of the infinite string loaded by N mass-spring systems located between $x=0$ and $x=L$.

and the location x_n are random variables. The system is then a disordered medium of propagation referred to as a disordered lattice. Several different situations must be considered: (i) The masses and/or the stiffnesses are a random variable but they are evenly located along the string ($x_{n+1} - x_n = d$). In this case we have to deal with a substitutional or cellular disorder. When we make random substitutions in a periodic lattice, we destroy the periodicity of physical parameters: some of them are no longer invariant under the translation group. Nevertheless, some quantities still remain sufficiently periodic to display the basic lattice; (ii) the location x_n is a random variable with $M_n = M$ and $k_n = k$. In this case, a topological or geometrical disorder arises; (iii) all the physical parameters are random variables, so we are dealing with a mixed disorder.

For the sake of simplicity, we consider that the nonlinearities are due only to the nonlinear terms in the stiffness of the spring; this implies that between two masses the trend for a transverse wave propagation is given simply by a linear equation. Each spring-mass system is governed by the equation of motion:

$$\begin{aligned} \frac{M_n}{T_s} \frac{\partial^2 y(x_n, t)}{\partial t^2} + \frac{1}{T_s} \frac{\partial U(x, t)}{\partial x} \Big|_{x=x_n} \\ = \frac{\partial y(x, t)}{\partial x} \Big|_{x=x_n^+} - \frac{\partial y(x, t)}{\partial x} \Big|_{x=x_n^-}, \end{aligned} \quad (1)$$

where T_s is the tension of the string and U is the potential of the restoring force. In the nonlinear case, the dynamic potential of the n th spring is

$$U(x_n, t) = \frac{1}{2} k_n y^2(x_n, t) + \frac{1}{4} \alpha_n k_n y^4(x_n, t) + O(y^5(x, t)), \quad (2)$$

where α_n describes the strength of the spring nonlinearity at the node x_n . We consider a harmonic time dependence wave such that

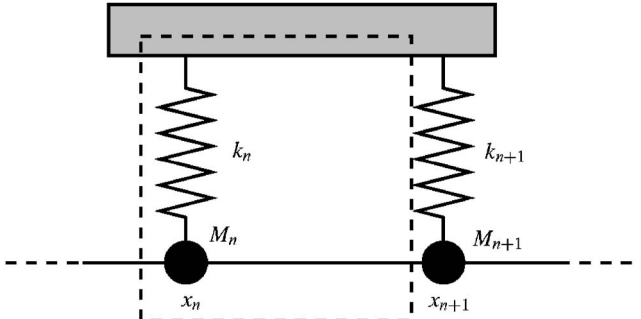


FIG. 2. Geometry of the n th cell.

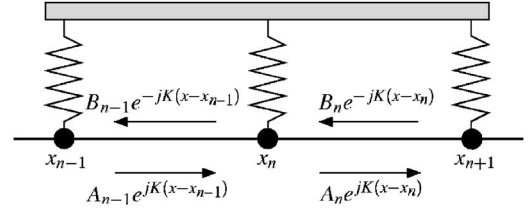


FIG. 3. A schematic representation of the conventional wave structure of a periodic loaded string.

$$y(x, t) = y(x) e^{j\omega t},$$

where ω is the angular frequency and we introduce the so-called “describing function method.” Although intensively used in atomic and condensed-matter physics [24], this approximation is also employed for mechanical modeling. In our case, the term $\cos^3(\omega t)$ is linearized as

$$\cos^3(\omega t) \approx \frac{3}{4} \cos(\omega t)$$

meaning that we focus only on the fundamental frequency. The influence of the higher harmonics has been investigated in [25,26]. We have shown that, as a first approximation, they may be neglected: in an acoustic lattice, the amplitude of the higher harmonics is typically 50 times smaller than the fundamental one.

The general propagation equation is

$$\frac{\partial^2 y(x)}{\partial x^2} + K^2 y(x) = \sum_{n=0}^N \delta(x - x_n) g_n(x) y(x), \quad (3)$$

where $K = \omega/c$ is the wave number with $c = \sqrt{T_s/\rho}$. In the above equation, $g_n(x)$ is now also dependent on the amplitude of the wave

$$g_n(x) = 1/\lambda_n \left[\left(1 - \frac{\omega^2}{\Omega_n^2} \right) + \frac{3}{4} \alpha_n y^2(x) \right],$$

where $\lambda_n = T_s/k_n$ and $\Omega_n^2 = k_n/M_n$. In the following, we assume that the nonlinearity coefficient α_n is a constant with respect to the position along the lattice, i.e., $\alpha_n = \alpha$ for all n .

III. GENERAL STUDY

The solution of Eq. (3) for $x_n \leq x \leq x_{n+1}$ is written as the sum of a forward (with amplitude A_n) and a backward (with amplitude B_n) wave (see Fig. 3) [23]. By using the continuity of the transverse displacement and the discontinuity of its first derivative at a resonator, we find, formally, the same system of equations as in the linear case (see Appendix A)

$$\begin{pmatrix} A_n \\ B_n \end{pmatrix} = \begin{pmatrix} (1 + u_n) e^{jKd_n} + u_n e^{-jKd_n} \\ -u_n e^{jKd_n} + (1 - u_n) e^{-jKd_n} \end{pmatrix} \begin{pmatrix} A_{n-1} \\ B_{n-1} \end{pmatrix} = \tilde{\mathbf{T}}_n \begin{pmatrix} A_{n-1} \\ B_{n-1} \end{pmatrix}, \quad (4)$$

where $u_n = 1/2jK\lambda_n(1 - \omega^2/\Omega_n^2) + \theta_n$. The nonlinear term θ_n depending on the wave intensity and on the position along the lattice is given by

$$\theta_n = \frac{3\alpha}{8jK\lambda_n} |A_{n-1}e^{jKd_n} + B_{n-1}e^{-jKd_n}|^2.$$

The nonlinear operator $\tilde{\mathbf{T}}_n$ gives the following formal expression for the propagation across a nonlinear lattice made up of N resonators:

$$\begin{pmatrix} A_N \\ B_N \end{pmatrix} = \prod_{n=1}^N \tilde{\mathbf{T}}_n \begin{pmatrix} A_0 \\ B_0 \end{pmatrix}, \quad (5)$$

where $(A_0, B_0)^t$ are the boundary conditions.

The waves outside the nonlinear structure can be described by [20]

$$y(x) = \begin{cases} R_i e^{jKx} + R_0 e^{-jKx} & \text{for } x \leq 0, \\ T_r e^{jK(x-x_N)} & \text{for } x > L, \end{cases} \quad (6)$$

where R_i , R_0 , and T_r are, respectively, the amplitude of the incident wave, the amplitude of the reflected wave, and the amplitude of the transmitted wave and where the total length of the lattice is $L=(N-1)d$. By determining the amplitude of the transmitted wave T_r (or A_N), the corresponding input amplitude R_i (or A_0) is found. So the nonlinear transmission coefficient $\tilde{\mathcal{T}}$ defined as

$$\tilde{\mathcal{T}} = \frac{|T_r|^2}{|R_i|^2} = \frac{|A_N|^2}{|A_0|^2}$$

is used to estimate the band structure.

The transmission problem can also be considered by means of an iterative nonlinear equation on $Y_n=y(x_n)$:

$$Y_{n+1} + Y_{n-1} - 2a_n Y_n + \Lambda_n |Y_n|^2 Y_n = 0 \text{ for } 0 < n \leq N, \quad (7)$$

where

$$a_n = \cos(Kd_n) + \frac{1}{2K\lambda_n} \left(1 - \frac{\omega^2}{\Omega_n^2} \right) \sin(Kd_n),$$

$$\Lambda_n = \frac{-3\alpha}{4K\lambda_n} \sin(Kd_n).$$

The propagation of a mechanical wave in the inhomogeneous medium with discrete nonlinearities can be studied in practice by means of these two approaches. For the case of weak nonlinearities in a periodic lattice, a perturbation method is used and we show that the presence of nonlinearities can improve the transparency of the medium. For the strong nonlinearity case, a general approach to the nonlinear problem is developed with the help of a nonlinear operator.

IV. THE PERTURBATION METHOD

To show how the nonlinearities modify the wave propagation, we first investigate the effects induced by one isolated nonlinearity. For a weak nonlinearity, the perturbation method leads to results consistent with numerical analysis. Then, for a low concentration of nonlinearities, the above results are extended to several nonlinear scatterers in the lattice.

A. The case of one nonlinearity

Consider an isolated nonlinearity placed at $x=x_0=0$ in a infinite uniform lattice. This nonlinearity is defined by the term $H[x_0, |Y(x_0)|] = H_0 = \Lambda_0 |Y(x_0)|^2$ in Eq. (7). When the amplitude of the wave is sufficiently small to consider the nonlinearity as a perturbation of the linear case, the Green's function of the perturbed string is written as (for $x_0=0$):

$$\begin{aligned} G(m, n, a) &= G_0(m, n, a) + \frac{G_0(m, 0, a) H_0 G_0(0, n, a)}{1 - H_0 G_0(0, 0, a)} \\ &= G_0(m, n, a) + G_0(m, 0, a) \Pi(a) G_0(0, n, a), \end{aligned} \quad (8)$$

where $\Pi(a)$ is the scattering operator and $G_0(m, n, a)$ is the Green's function of the ordered linear lattice given by (see Appendix B)

$$G_0(m, n, a) = \frac{-(a - \sqrt{a^2 - 1})^{|m-n|}}{2\sqrt{a^2 - 1}}.$$

$G_0(m, n, a)$ is interpreted as the wave amplitude at the node x_n when the unit force source is located at x_m . For a periodic lattice, with parameter

$$a = \cos(Kd) + \frac{1}{2K\lambda} \left(1 - \frac{\omega^2}{\Omega^2} \right) \sin(Kd),$$

the Green's function G_0 is defined as the solution of the inhomogeneous discrete equation:

$$G_0(m, n+1, a) - 2aG_0(m, n, a) + G_0(m, n-1, a) = \delta_{m,n}, \quad (9)$$

where $\delta_{m,n}$ is the Kronecker delta.

Two different propagation behaviors (stopband and passband) are considered and the Green's function is determined for each case.

1. The evanescent mode (stopband)

The pole of the Green's function given by

$$G_0(m, n, a) = 1/[\Lambda_0 |Y(x_0)|^2]$$

is outside a passband since $\Lambda_0 |Y(x_0)|^2$ is real. The value a_p of the parameter a corresponding to this pole is

$$a_p = \sqrt{1 + \frac{1}{4}\Lambda_0^2 |Y(x_0)|^4}$$

and the magnitude of this evanescent mode $Y(x_0)$ is found with the help of the residue of the Green's function for $a=a_p$:

$$|Y(x_n)^{(p)}|^2 = \text{Res}[G(m, n, a_p)].$$

For $n=0$ and using the equation of the Green's function in the unperturbed linear case, the amplitude is written as

$$|Y(x_0)^{(p)}|^2 = 2 \sqrt{1 - \left(\frac{1}{\Lambda_0} \right)^2},$$

and the vibration amplitude at point $x_n=nd$ is given by

$$|Y(x_n)| = |Y(x_0)^{(p)}| (|\Lambda_0| - \sqrt{\Lambda_0^2 - 1})^n$$

$$=|Y(x_0)^{(p)}|e^{n \ln(|\Lambda_0| - \sqrt{\Lambda_0^2 - 1})}.$$

For $|\Lambda_0| < 1$, the amplitude $|Y(x_n)|$ has a complex form what shows the propagative nature of the mode. This result is completely opposed to that of the linear case, where an evanescent mode is present for the same value of a . So, a mode belonging to the forbidden band in the linear case becomes propagative with the presence of one nonlinearity in an ordered lattice. Conversely, for $|\Lambda_0| > 1$, propagation is impossible and the corresponding evanescent mode decreases exponentially in the vicinity of the nonlinearity location with the localization length ξ :

$$\xi = -\frac{d}{\ln(|\Lambda_0| - \sqrt{\Lambda_0^2 - 1})}.$$

2. The propagative mode (passband)

When $|a| \leq 1$, all the modes are propagative (Green's function does not have any pole). The amplitude of the mode at a given node of the lattice results in the convolution product of the excitation and the Green's function in the perturbed case. The energy transmission coefficient t of the nonlinearity is given by the relation [27]

$$t = \frac{1}{|1 - \Lambda_0 Y(x_0)|^2 G_0(0,0,a)^2},$$

where the Green's function element $G_0(0,0,a)$ is given by $G_0(0,0,a) = (-j)/\sqrt{1-a^2}$. Finally, by setting $a = \cos(qd)$ t is the solution of the cubic equation:

$$t^3 \Lambda_0^2 + t \sin^2(qd) - \sin^2(qd) = 0.$$

This third order equation can be numerically processed to illustrate the behavior of the system with localized nonlinearity and to show its influence on the transparency of the medium.

B. The case of several nonlinearities

When p consecutive nonlinearities are present in the lattice, the perturbation is written as

$$H_p = \sum_{i=0}^{p-1} \Lambda_i |Y(x_i)|^2,$$

and the Green's function of the string is given by the recursive relation:

$$G_p(m,n,a) = G_{p-1}(m,n,a) + \frac{G_{p-1}(m,p-1,a) \Lambda_{p-1} |Y(x_{p-1})|^2 G_{p-1}(p-1,n,a)}{1 - \Lambda_{p-1} |Y(x_{p-1})|^2 G_0(p-1,p-1,a)}.$$

If $|\Lambda_i| < 1$, for $i=1, \dots, p$, all the modes are propagative in the lattice with a finite number of discontinuities. In the opposite case, the modes are evanescent and the medium is completely opaque. So the theory of the Green's function and the perturbation method show that a wave with a small amplitude and with a frequency within a stopband of the

linear lattice can propagate in a medium with weak nonlinearities.

V. TRANSPARENCY OF THE NONLINEAR LATTICE FOR LOW FREQUENCIES

To address quantitatively the question of what happens in the low-frequency range regime, let us approach the problem physically by following the amplitude trend of the wave injected into the nonlinear lattice. By letting

$$\phi_n = A_n + B_n,$$

$$\psi_n = A_n - B_n,$$

and with the low-frequency hypothesis ($Kd \ll 1$), Eq. (4) becomes

$$\phi_n = \phi_{n-1} - jKd_n \psi_n,$$

$$\psi_n = \psi_{n-1} - jKd_n \phi_n - 2u_n \phi_n,$$

where $u_n = 1/(2jK\lambda_n)(1 - \omega^2/\Omega_n^2) + 3\alpha/(8jK\lambda)|\phi_n|^2$. In the continuum form, these equations are

$$\frac{d\phi(n)}{dn} = -jK\psi(n),$$

$$\frac{d\psi(n)}{dn} = -jK\phi(n) - \frac{2u_n}{d}\phi(n).$$

$\phi(n)$ is then the solution of the following equation:

$$\frac{d^2\phi(n)}{dn^2} = -\left[K^2 - \frac{2jK}{d}u_n\right]\phi(n) = -\beta^2\phi(n), \quad (10)$$

where d is the mean value of d_n . If we look for a traveling wave having the form $\phi(n) = \phi(N)e^{-j\beta(N-n)d} = T_r e^{-j\beta(N-n)d}$, we find

$$\beta^2 = \frac{K^2}{d^2} - \frac{1}{d^3\lambda} \left(1 - \frac{\omega^2}{\Omega^2}\right) - \frac{3\alpha}{4d^3\lambda} |T_r|^2 \quad \text{for } \alpha \geq 0,$$

$$\beta^2 = \frac{K^2}{d^2} - \frac{1}{d^3\lambda} \left(1 - \frac{\omega^2}{\Omega^2}\right) + \frac{3\alpha}{4d^3\lambda} |T_r|^2 \quad \text{for } \alpha \leq 0,$$

where λ and Ω are the mean values of λ_n and Ω_n . The transmission of the wave essentially depends on the sign of β^2 , i.e., the transmitted intensity $|T_r|^2$. When $\beta^2 > 0$, the wave is propagative. The value

$$|T_r| = \sqrt{\frac{4[K^2d - 1/\lambda(1 - \omega^2/\Omega^2)]}{3\alpha\lambda}} \quad (11)$$

characterizes the boundary between the propagative and the nonpropagative regimes. The nonlinear term narrows the passband width when $\alpha > 0$ and, conversely, the nonlinearities change a stopband into a passband for $\alpha < 0$. These results reinforce the idea of a competition between the effects of the disorder and those of the nonlinearities in the wave propagation process.

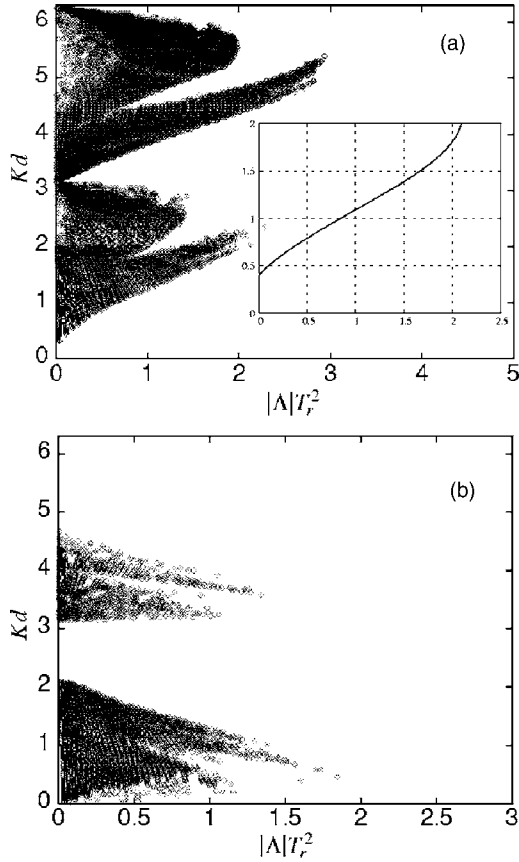


FIG. 4. Phase diagram with a positive nonlinearity $\alpha > 0$ [(a)] and a negative one $\alpha < 0$ [(b)]. The inset shows the boundary line between the propagative and the nonpropagative regime resulting from the Eq. (11).

VI. NUMERICAL RESULTS

By using the inverse of the nonlinear relation (5), the propagation of a mechanical wave through a lattice made up of N nonlinear resonators is simulated. The inverse of Eq. (5) is used to avoid divergent and bifurcation problems due to the nonlinearities (the multistability phenomenon comes into play in the calculation of the transmitted wave).

In contrast to the linear case, the transmission coefficient depends on the amplitude of the input wave. Several cases with different initial conditions are considered. To express the similarity between the mean of the magnitudes of the nonlinearity Λ and the intensity of the wave Y_n^2 , the variable $|\Lambda|T_r^2$ is introduced as a measure of the nonlinearity.

To determine the allowed and forbidden bands, we proceed as follows. For a fixed value of the frequency Kd the amplitude of the transmitted wave is chosen. The recurrence formula (7) is used to calculate the amplitude of the incident wave. If the ratio \tilde{T} given by

$$\tilde{T} = \frac{|T_r|^2}{|R_i|^2}$$

is higher (lower) than a threshold (in our case $\tilde{T}_{lim} = 0.6$) the frequency belongs to allowed (forbidden) bands. The relevant physical quantity may be described by representing the

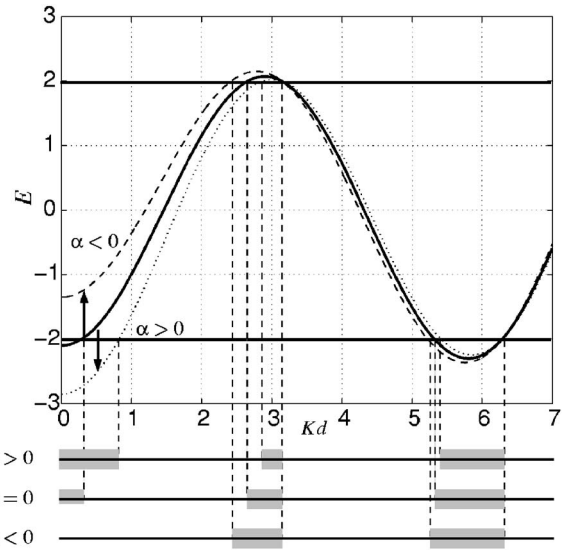


FIG. 5. $E = -2a + \Lambda|Y_n|^2$ vs Kd for the linear case (solid line), positive nonlinear case (dotted line), and negative nonlinear case (dashed line). The forbidden bands in the different cases are illustrated by the hatched parts under the graph.

dimensionless frequency Kd versus the variable $|\Lambda|T_r^2$. Each point on the graph is defined for a given frequency and a value of $|\Lambda|T_r^2$. A point in the black-colored area corresponds to an allowed band (a propagative mode), otherwise a point in the white-colored area is a signature of a forbidden band (a localized mode).

A. The periodic lattice case

The analysis of Fig. 4 shows that the nonlinearities perturb the band structure of the lattice. The behavior of the propagation is not as simple as in the linear case and a wide range of situations has to be considered. The comparison of Figs. 4(a) and 4(b) reveals the importance of the sign of the nonlinearity: for $\alpha > 0$ [Fig. 4(a)], the width of the first stopband (low frequencies) increases but the second and third ones fully disappear; the first allowed band gets narrower, increasing the opacity of the lattice in this frequency range; for $\alpha < 0$ [Fig. 4(b)] the first allowed band stretches.

These results are confirmed by a qualitative analysis resulting from the recursive equation

$$Y_{n+1} + Y_{n-1} + (-2a + \Lambda|Y_n|^2)Y_n = 0.$$

In the linear case ($\alpha = 0$), the allowed bands are given by the condition $-1 \leq a \leq 1$. By analogy, for low wave amplitude Y_n the value of $-2a + \Lambda|Y_n|^2$ gives the qualitative behavior of the propagation regime. Figure 5 shows how the cutoff frequencies move when

$$-2a \rightarrow -2a + \Lambda|Y_n|^2$$

for $\alpha > 0$ and $\alpha < 0$ as a function of Kd (for $Y_n = 1$).

When $\alpha < 0$, the first stopband disappears because $-2a + \Lambda|Y_n|^2$ becomes greater than -2 , but, on the contrary, for $\alpha > 0$, the width of this stopband increases. For the second stopband, $-2a + \Lambda|Y_n|^2$ becomes smaller than 2 for $\alpha > 0$, but

greater than 2 for $\alpha < 0$ and the tendency is reversed. The presence of nonlinearities can change the regime of the propagation according to its sign and the frequency. Some stopbands can become passbands but conversely some passbands can become stopbands. All these results are confirmed by the simulation [Fig. 4].

For $\alpha > 0$ the comparison of the simulation results with the analytical results [inlet Fig. 4(a)] resulting from Eq. (11) in the low-frequency approximation shows the validity of this approach. It is also worth noting that the value of $|\Lambda|T_r^2$, resulting from the relation (11), does not depend on the value of the nonlinearity:

$$|\Lambda|T_r^2 = |\sin(Kd)| \left[Kd - \frac{1}{K\lambda} \left(1 - \frac{\omega^2}{\Omega^2} \right) \right].$$

In other words, for low frequencies, positive nonlinearities lead to a decrease of the passband width, whatever their strengths.

The second important nonlinear effect is multistability. Indeed, for some frequency values, a gap in the propagative regime appears in relation with the magnitude of $|\Lambda|T_r^2$. Figures 6(a) and 6(b) illustrate two examples of this phenomenon, one for a corresponding passband in the linear case [Fig. 6(a)] and the other belonging to a stopband [Fig. 6(b)]. These responses are a manifestation of the multistability and are directly connected to the chaotic nature of the wave propagation in such a medium. In some circumstances, the nonlinearities transform a stable regime (passband) into an unstable one (stopband) and vice versa. Several changes of regime can induce a chaotic situation synonymous with full opacity.

In short, the nonlinearities with a well-chosen sign and for low wave intensity increase the transparency in the case of a frequency belonging to a passband (linear case) and reduce the share of the stopbands. Conversely, for high intensity, no transmission is possible and the medium becomes opaque for almost all frequencies. For a periodic nonlinear lattice, two important results are, first, that the sign of the nonlinearity has a great influence on the nature of the wave propagation in the medium and, second, that these nonlinearities can be the cause of chaotic behavior which prevents any propagation.

B. The disordered lattice case

In this section, special attention is given to the coexistence of nonlinearities and disorder. The nonlinear operator formalism is used to simulate the propagation of a mechanical wave through a disordered lattice. The interactions between nonlinearities and disorder are examined. Two situations are studied: cellular and topological disorders with the same nonlinearity for each resonator ($\alpha > 0$).

Figure 7 shows the disorder effects: (i) disorder restricts the passband width with respect to the ordered linear case and destroys the band structure. As in the linear case, the effect of topological disorder [Fig. 7(b)] is more efficient than that of cellular disorder [Fig. 7(a)]. Nevertheless, the nonlinearities can counteract the disorder effect for large wave amplitudes associated with low frequencies: (ii) the

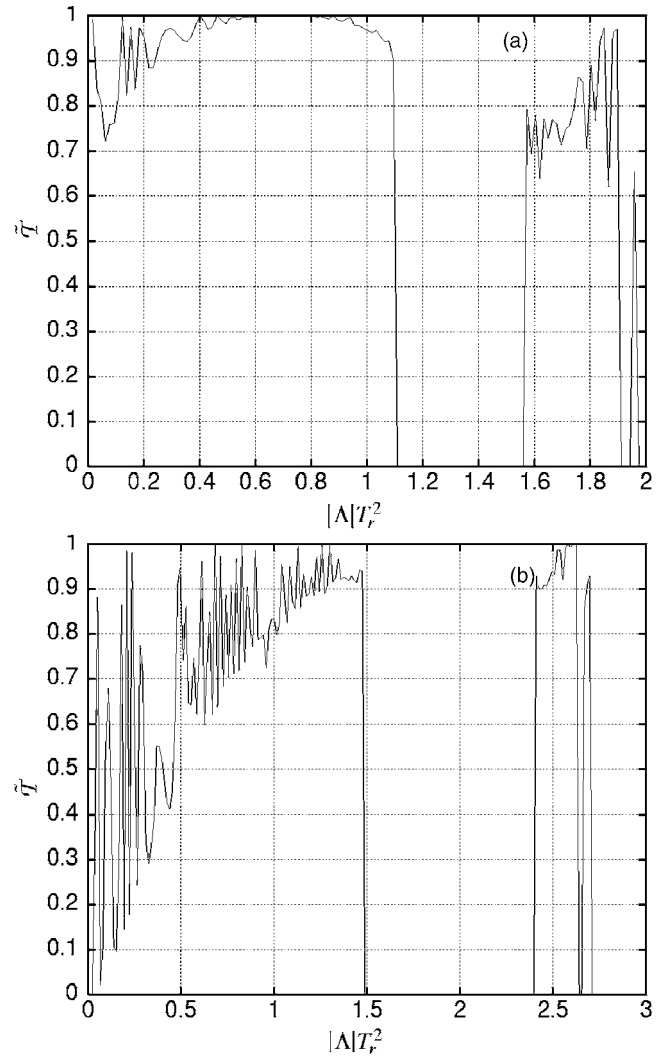


FIG. 6. Transmission coefficient versus $|\Lambda|T_r^2$ for $Kd=2.1$ (a) and for $Kd=5$ (b).

second stopband of the linear case (between $Kd=2.2$ to $Kd=\pi$) almost disappears, regardless of the type of disorder [Figs. 7(a) and 7(b)].

To illustrate this remark, the transmission coefficient is plotted for a particular frequency as a function of lattice length in Fig. 8. In the linear case, this coefficient depends on the localization length ξ through the relation [28]

$$\mathcal{T} = e^{-L/\xi}.$$

In the nonlinear case, the nonlinear transmission coefficient behaves as (see Fig. 8):

$$\tilde{\mathcal{T}} \sim L^{-\frac{1}{\xi(\alpha)}}$$

since it is represented by a line in the same reference. In this case, the localization length $\xi(\alpha)$ depends weakly on the strength of the nonlinearity α as Fig. 8 shows.

The nonlinearities act as a factor of delocalization because the localization length increases with nonlinearity. It must be noted however that the Anderson localization overcomes the effects of nonlinearity for high frequency: the lattice stays or

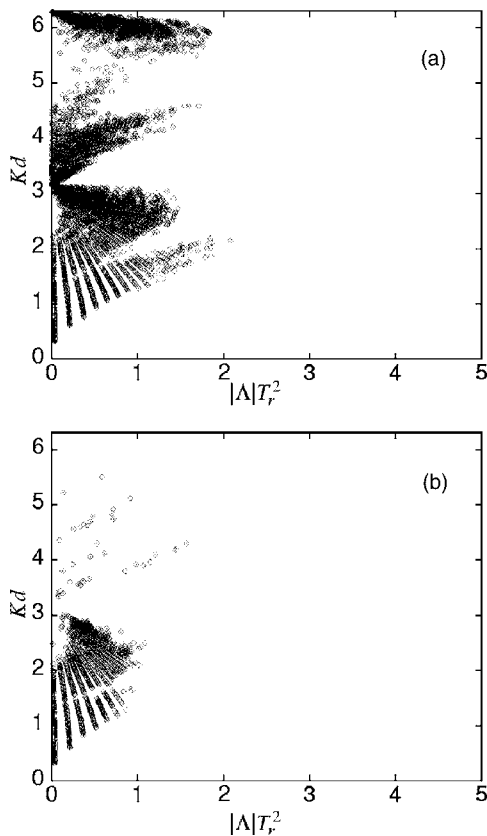


FIG. 7. Phase diagram with a cellular disorder (a) and a topological disorder (b) with a standard deviation $\sigma=0.1$.

becomes opaque as in the linear case. The same conclusions apply when the strength of the disorder is high: no wave propagates through the medium, even for low frequency.

To conclude this section, we shall now sum up the major results. We have shown that the presence of nonlinearity increases the transparency of the lattice for a low-strength disorder. Nevertheless, the nonlinear behavior of the medium does not preclude the general decrease of transmittivity and Anderson localization for a high-strength disorder. The multistability phenomenon is always present, with the disorder

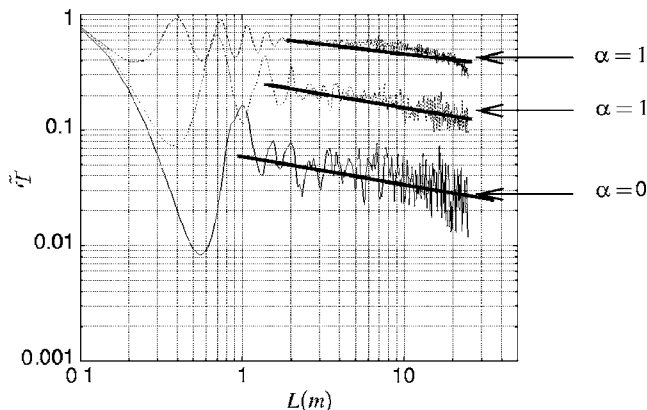


FIG. 8. Transmission coefficient with disorder on masses ($\sigma = 10$) vs the lattice length for $Kd=2.4$ and with $\alpha=10$, $\alpha=1$, $\alpha=0.1$.

showing the effective role of nonlinearity in the low-frequency domain and the need for an approach to describe this aspect of the propagation. A nonlinear discrete map is developed in the following section to study the disorder effect on this nonlinear phenomenon.

VII. NONLINEAR DISCRETE MAPPING

In this section, we investigated how the wave moves through the lattice considered as a dynamic system. Similar studies have been worked out in solid state physics [23,29–36].

When we speak of a dynamic system, we understand something like an n -particle system characterized at any time by their positions and momenta. The state of this system is specified as a point in a $2n$ -dimensional phase space in which the observable quantities of the system such as energy are smooth real-valued functions. When the dynamic system evolves, it is subject to constraints due to the constants of the motion, so its representative point evolves only in a submanifold of the phase space. Depending on the behavior of the system, the trajectory of the representative point is a closed trajectory (limit circle), a trajectory rolled up around a torus or an aperiodic solution of the system.

Our approach uses the finite difference Eqs. (7), which link together the values of the wave function at three consecutive nodes of the lattice. From the real and imaginary parts of the wave function

$$\chi_n = x_n + jy_n$$

we get a system of two coupled equations. The wave is then represented as a point in a four-dimensional space, the coordinates of which are $(x_{n-1}, x_n, y_{n-1}, y_n)$. This space is interpreted as the phase space of the wave seen as a dynamic system.

When the wave runs through the lattice, localizing the trajectory of its representative point gives important information about the constants of the motion. To make it easier to analyze how the wave moves through the lattice, we consider its Poincaré section, which is a mapping of the intersections of its trajectory in the phase space with a plane. For example, for a wave traveling in a linear periodic lattice, the Poincaré section reduces to a single point. This map is characterized by two control parameters: the wave number K and the intensity of the incidence wave. In this plane, the solutions of the propagation equation are represented by orbits which describe the propagation regime.

The orbits generated by the intersection of the trajectory with the plane can be either bounded or unbounded. Only those from the first category contribute to the transmission (corresponding to a passband frequency). The bounded orbits (closed curves) are organized into quasiperiodic orbits of different periods (called n -periodic orbits where n is the number of periods). Conversely, the unbounded orbits are synonymous with an aperiodic trajectory and describe a wave which does not propagate through the lattice.

A. Mathematical formalism

The first equation of system (7), written in terms of real and imaginary parts of the transverse amplitude Y_n , repre-

sents a nonlinear system defined in a four-dimensional space. Letting $Y_n = \kappa_n e^{j\gamma_n}$, we find

$$\begin{aligned} \kappa_{n+1} \cos(\Delta \gamma_{n+1}) + \kappa_{n-1} \cos(\Delta \gamma_{n-1}) &= 2f_n(\kappa_n), \\ \kappa_{n+1} \sin(\Delta \gamma_{n+1}) + \kappa_{n-1} \sin(\Delta \gamma_{n-1}) &= 0, \end{aligned} \quad (12)$$

where $\Delta \gamma_n = \gamma_n - \gamma_{n-1}$ and $f_n(x) = \frac{1}{2}x(\Lambda_n x^2 - 2a_n)$. The second equation of this system provides an invariant of motion

$$J_n = \frac{-i}{2}(Y_n^* Y_{n+1} - Y_{n+1}^* Y_n) = \kappa_n \kappa_{n+1} \sin(\Delta \gamma_{n+1}) \quad (13)$$

and allows the nonlinear mapping to be reduced from four to two dimensions. Using the variable $v_n = \frac{1}{2}(Y_n^* Y_{n+1} + Y_{n+1}^* Y_n)$, the nonlinear transmission problem is described by mapping H :

$$H: \begin{cases} \kappa_{n-1}^2 = \frac{1}{\kappa_n^2}(v_n^2 + J_n^2), \\ v_{n-1} = -v_n - \kappa_{n-1}^2(\Lambda_n \kappa_{n-1}^2 - 2a_n). \end{cases} \quad (14)$$

With the variables $p_n = \frac{1}{2}\Lambda_n \kappa_n^2$ and $q_n = v_n / \kappa_n^2 + \frac{1}{2}(-2a_n + \Lambda_n \kappa_n^2)$, the mapping H is area-preserving and symmetrical [31]

$$H: \begin{cases} p_{n-1} = p_n(-a_n + p_n + q_n)^2 + \frac{(\Lambda_n J_n)^2}{p_n}, \\ q_{n-1} = -q_n + \left(1 - \frac{p_n}{p_{n-1}}\right)(-a_n + p_n + q_n + p_{n-1}). \end{cases} \quad (15)$$

The orbits corresponding to this mapping in the phase plane (p_n, q_n) are built. They are similar to the Poincaré section of the nonlinear dynamic system, where n plays the role of a discrete time.

Starting from the ‘‘initial’’ conditions Y_{N+1} and Y_N , we obtain κ_{N+1} and κ_N , which lead to the invariant J_N and to v_n . Using the system (15), we go back to the origin of the motion ($n=0$) and the transmission coefficient \tilde{T} can be estimated.

With this method, two possibilities are available for illustrating the propagation through a nonlinear lattice: the calculation of the transmission coefficient or the building of the Poincaré section.

B. Numerical results

In order to examine the nonlinear transmission problem in more detail, two typical cases are described in the (p_n, q_n) plane and the results are shown in Figs. 9 and 10 for an ordered lattice. In these figures, the transmission is linked with orbits which are bounded (transmitted waves) or diverging (localized waves). Each orbit corresponds to a different value of $|\Lambda|T_r^2$: we proceed by fixing the output T_r^2 and calculate the corresponding p_n and q_n for each value of n .

Figure 9 presents the orbits for a propagative wave with a frequency $Kd=4.21$ corresponding to a linear passband. For a weak amplitude, the curves at the left of the figure are

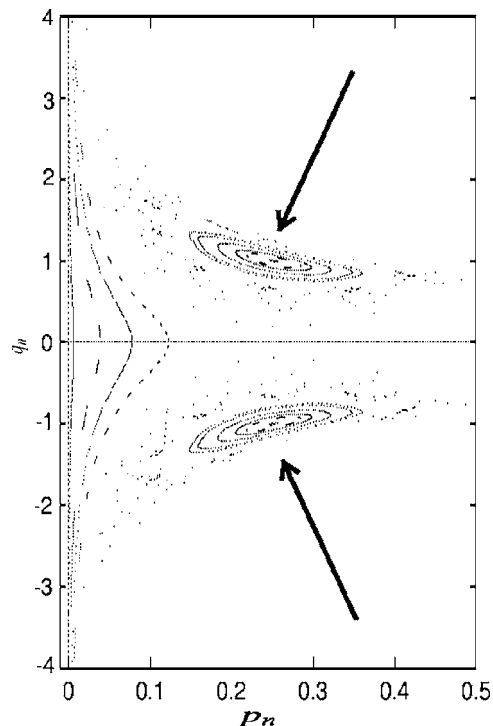


FIG. 9. Some of orbits corresponding to values of $|\Lambda|T_r^2$ for $Kd=4.21$ in the (p_n, q_n) plane for the nonlinear ordered case.

bounded, showing one-periodic or quasiperiodic behavior synonymous of propagation through the lattice.

From the value $|\Lambda|T_r^2=0.7$, the orbits have unstable behavior and no longer display any periodicity (the points are almost randomly distributed). This zone corresponding to $0.7 \leq |\Lambda|T_r^2 \leq 0.9$ corresponds to a gap in the transmission [see the phase diagram in Fig. 4(a)] and represents a forbidden band (evanescent wave). For $|\Lambda|T_r^2 > 0.9$, the orbits return to periodic behavior with a double period (two-periodic): two attraction basins are present and are indicated by arrows. This phenomenon shows the existence of a bifurcation during the unstable behavior.

For higher values of the $|\Lambda|T_r^2$ parameter, the two-periodic orbits are unstable, leading to a stochastic behavior associated with the opacity of the medium. This shows that nonlinearities can transform a region which is stable in the linear case into an unstable region.

Figure 10(a) shows the results for a frequency $Kd=2.5$ corresponding to a linear stopband. In this case, nonlinearities transform unstable orbits corresponding to a stopband into stable ones corresponding to a passband. The stable one-periodic orbits are surrounded by four-periodic orbits (see arrows) which become chaotic and lose their stability. In this case, there is no gap in the transmission but the difference between the two sorts of transmittive waves can be observed with this illustration. Generally, this change of period precedes a transmission loss (see Fig. 6) because the two- or four-periodic orbits are less stable than the one-periodic ones. This example illustrates how the representation of the wave in the phase space gives an insight into the various propagation properties of the medium.

The effect of the disorder on the transmission may also be observed from the Poincaré sections. In this case, we con-

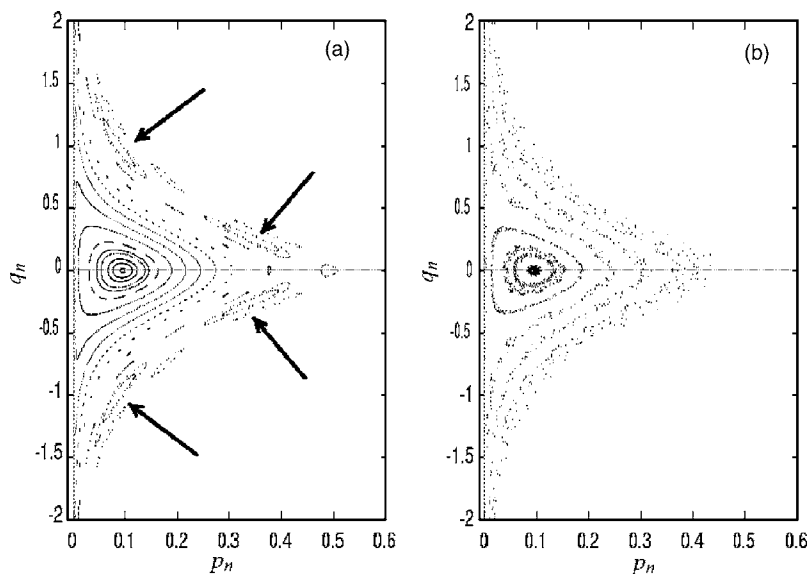


FIG. 10. (a) Some of orbits corresponding to values of $|\Lambda|T^2$ for $Kd=2.5$ in the (p_n, q_n) plane for the nonlinear ordered case. (b) Corresponding case of (a) with a small cellular disorder.

consider only a weak disorder to assume that J_n is a constant of motion (at least as a mean value). For a wave propagating in a nonlinear lattice with a small amount of disorder, the Poincaré section has the same global structure as the ordered case, but is now blurred. Figure 10(b) illustrates such a result: the orbits of Fig. 10(a) are spread out by the effects of the disorder. This means that a weak disorder perturbs the transmission through the medium but does not prevent it. In the same way, we observe from the numerical simulations that the orbits lose their stability more easily with disorder than without disorder.

These results are in good agreement with those of the previous section: the effect of the disorder is attenuated by nonlinearities as long as its strength is not too high, whereas for strong disorder, the Anderson localization overrides the nonlinear effects.

VIII. CONCLUSION

In the present paper, we have studied the relationship between disorder and nonlinearity in a wave propagating through a quasi-one-dimensional string loaded by resonators. On the basis of numerical simulations carried out on relevant physical parameters, particular conclusions have been obtained on the band spectrum of the vibrating modes.

Nonlinearity exhibits more complex features, depending on a variety of parameters such as the magnitude of the nonlinearity and the amplitude of the waves. For some frequencies, nonlinearity increases the transparency of the medium without perturbing the other transmitting frequencies in the small nonlinearity or amplitude regime.

Generally, the presence of nonlinearities acts as a factor of delocalization when the sign of the nonlinearity is well chosen. In an ordered lattice, it is clearly shown that the transmission coefficient increases and, with the help of a nonlinear discrete mapping, we have demonstrated the existence of several sorts of transmitted waves with various degrees of stability. For the disordered case, with a low-strength disorder, the transmission is increased by the presence of nonlin-

earities. For higher frequencies, these effects are less efficient and this trend is accentuated when the strength of disorder increases.

By adjusting the various parameters which govern the complicated competition between the effects of disorder and nonlinearities on wave propagation, we hope to control the flow of acoustic or mechanical energy through a large structure.

APPENDIX A: PROPAGATION IN A PERIODIC LINEAR LATTICE

In an ordered lattice, all the physical quantities are independent of their position and so the medium is periodic with the periodicity $d=x_{n+1}-x_n$. In the n th cell (for $x_n \leq x \leq x_{n+1}$), the amplitude of the wave is the contribution of forward and backward waves with respective amplitudes A_n and B_n :

$$y(x) = A_n e^{jK(x-x_n)} + B_n e^{-jK(x-x_n)}.$$

The matching conditions for the function $y(x)$ and its first derivative at the nodes x_n lead to the recurrence relations:

$$A_n = (1+u)A_{n-1}e^{jKd} + uB_{n-1}e^{-jKd},$$

$$B_n = -uA_{n-1}e^{jKd} + (1-u)B_{n-1}e^{-jKd}, \quad (\text{A1})$$

where $u=1/(2jK\lambda)(1-\omega^2/\Omega^2)$. This system (A1) may be written in matrix form as

$$\begin{bmatrix} A_{n+1} \\ B_{n+1} \end{bmatrix} = \begin{bmatrix} (1+u)e^{jKd} & ue^{-jKd} \\ -ue^{jKd} & (1-u)e^{-jKd} \end{bmatrix} \begin{bmatrix} A_n \\ B_n \end{bmatrix} = \mathbf{T} \begin{bmatrix} A_n \\ B_n \end{bmatrix}, \quad (\text{A2})$$

where \mathbf{T} is the propagation matrix modeling the transmission across a cell. The elements of \mathbf{T} depend on the frequency in two ways: through the wave number of the string $K(\omega)$ and through the frequency dependence of the scatterer (λ and Ω). The reciprocity principle and the fact that the system is non-dissipative lead to the relations $\det \mathbf{T}=1$ and

$\mathbf{T}_{22}=\mathbf{T}_{11}^*$ for the propagation matrix. The forward and backward wave amplitudes in the n th cell determine the traveling wave amplitudes in any other cell of the lattice by the repeated application of \mathbf{T} or \mathbf{T}^{-1} .

The general propagation problem in the lattice between nodes n and m is then described by the iteration of $(n-m)$ \mathbf{T} matrices

$$\begin{bmatrix} A_n \\ B_n \end{bmatrix} = \mathbf{T}^{(n-m)} \begin{bmatrix} A_m \\ B_m \end{bmatrix}, \quad (\text{A3})$$

where $(A_m, B_m)^t$ can be considered as a boundary condition. The eigenvalues of \mathbf{T}^{n-m} , which depend on the frequency and on the parameters of the lattice, give the behavior of the waves through the dispersion relation of the wave [37].

APPENDIX B: CALCULATION OF THE GREEN FUNCTION FOR THE LINEAR ORDERED CASE

The Green function verifies the equation

$$G_0(m, n+1, a) + G_0(m, n-1, a) - 2aG_0(m, n, a) = \delta_{m,n}. \quad (\text{B1})$$

We set

$$G_0(m, n, a) = \frac{1}{2\pi} \int_{-\pi}^{+\pi} \tilde{G}(\theta) e^{j(m-n)\theta} d\theta,$$

and

$$\delta_{m,n} = \frac{1}{2\pi} \int_{-\pi}^{+\pi} e^{j(m-n)\theta} d\theta, \quad (\text{B2})$$

where $\tilde{G}(\theta)$ represents the Fourier transform. Using Eq. (B1) we obtain

$$G_0(m, n, a) = \frac{1}{2\pi} \int_{-\pi}^{+\pi} \frac{e^{j(m-n)\theta}}{2[\cos(\theta) - a]} d\theta. \quad (\text{B3})$$

The residue theorem allows us to calculate $G_0(m, n, a)$ by an integration in the complex plane. Setting $z=e^{j\theta}$ and $d\theta = -jdz/z$, we find

$$G_0(m, n, a) = \frac{-j}{2\pi} \int_C \frac{z^{m-n}}{z^2 - 2az + 1} dz, \quad (\text{B4})$$

where C is the unit circle. Using the residue theorem, we find

$$\int_C f(z) dz = 2j\pi \text{Res}[f(z)],$$

with

$$f(z) = \frac{z^{m-n}}{z^2 - 2az + 1}. \quad (\text{B5})$$

Only the pole such that $|z| < 1$ contributes to the integral. In this case, one has only one pole

$$z_p = a - \sqrt{a^2 - 1}$$

and

$$\text{Res}[f(z)] = \lim_{z \rightarrow z_p} (z - z_p) f(z) = \lim_{z \rightarrow z_p} (z - z_p) \frac{z^{m-n}}{(z - z_p)(z + z_p)}.$$

Finally, by using Eq. (B4), we find the expression of the Green function, for the linear ordered case:

$$G_0(m, n, a) = -\frac{(a - \sqrt{a^2 - 1})^{|m-n|}}{2\sqrt{a^2 - 1}}. \quad (\text{B6})$$

-
- [1] P. W. Anderson, Phys. Rev. **109**, 1492 (1958).
 [2] P. Sheng, *Scattering and Localization of Classical Waves in Random Media* (Singapore, World Scientific, 1990).
 [3] A. Sánchez, E. Macià, and F. Dominguez Adame, Phys. Rev. B **49**, 15428 (1994).
 [4] A. Sanchez, F. Dominguez Adame, G. Berman, and F. Izrailev, Phys. Rev. B **51**, 6769 (1995).
 [5] C. M. Soukoulis, S. Datta, and E. N. Economou, Phys. Rev. B **49**, 3800 (1994).
 [6] Yu S. Kivshar, S. A. Gredeskul, A. Sanchez, and L. Vasquez, Phys. Rev. Lett. **64**, 1693 (1990).
 [7] E. Cota, J. V. Jose, J. Maytorena, and G. Monsivais, Phys. Rev. Lett. **74**, 3302 (1995).
 [8] P. Devillard and B. Souillard, J. Stat. Phys. **43**, 423 (1986).
 [9] M. Sayar, M. C. Demirel, and A. R. Atilgan, J. Sound Vib. **205**, 372 (1997).
 [10] M. J. McKenna, J. Keat, J. Wang, and J. D. Maynard, Physica B **194**, 1039 (1994).
 [11] M. J. McKenna, R. L. Stanley, and J. D. Maynard, Phys. Rev. Lett. **69**, 1807 (1992).
 [12] D. L. Shepelyansky, Phys. Rev. Lett. **70**, 1787 (1993).
 [13] A. A. Zevin, J. Sound Vib. **193**, 847 (1996).
 [14] R. Spigler, J. Math. Phys. **27**, 1760 (1996).
 [15] D. J. Mead and S. M. Lee, J. Sound Vib. **92**, 427 (1984).
 [16] R. Knapp, G. Papanicolaou, and B. White, Nonlinearity and Localization in One-dimensional Random Media, edited by A. R. Bishop, D. K. Campbell, and St. Pnevmatikos, *Disorder and nonlinearity*, Springer Series in Solid State Science (Springer, Berlin 1989).
 [17] R. Knapp, G. Papanicolaou, and B. White, J. Stat. Phys. **63**, 567 (1991).
 [18] C. M. Soukoulis, Jorge V. José, E. N. Economou, and P. Sheng, Phys. Rev. Lett. **50**, 764 (1983).
 [19] M. Luban and J. H. Luscombe, Phys. Rev. B **34**, 3674 (1986).
 [20] S. A. Gredeskul and Y. S. Kivshar, Phys. Rep. **216**, 1 (1992).
 [21] V. V. Beloshapkin, A. G. Tretyakov, and G. M. Zaslavsky, Commun. Pure Appl. Math. **47**, 39 (1994).
 [22] C. W. Cai, H. C. Chan, and Y. K. Cheung, Trans. ASME, J. Appl. Mech. **64**, 940 (1997).
 [23] D. Hennig, H. Gabriel, and G. P. Tsironis, Phys. Rep. **307**, 333 (1999).
 [24] R. Loudon, *The Quantum Theory of Light* (Clarendon, Oxford,

- 1983).
- [25] O. Richoux, C. Depollier, and J. Hardy, *Acta. Acust. Acust.* **88**, 934 (2002).
- [26] G. Gonon, O. Richoux, and C. Depollier, *Signal Process.* **83**, 2469 (2003).
- [27] O. Richoux, Thèse de doctorat, Université du Maine, 1999 (unpublished).
- [28] J. M. Luck, *Systèmes Désordonnés Unidimensionnels* (Collection Alea Saclay, 1992).
- [29] Y. Wan and C. M. Soukoulis, *Phys. Rev. A* **41**, 800 (1990).
- [30] Y. Wan and C. M. Soukoulis, in *Wave Transmission in a One-Dimensional Nonlinear Lattice: Multistability and Noise*, edited by A. R. Bishop, *Springer Proceedings in Physics: Disorder and Nonlinearity* Vol. 39 (Springer-Verlag, Berlin, 1989).
- [31] M. Grabowski and P. Hawrylak, *Phys. Rev. B* **41**, 5783 (1990).
- [32] P. Hawrylak, M. Grabowski, and P. Wilson, *Phys. Rev. B* **40**, 6398 (1989).
- [33] P. Hawrylak and M. Grabowski, *Phys. Rev. B* **40**, 8013 (1989).
- [34] F. Delion, Y. E. Levy, and B. Souillard, *Phys. Rev. Lett.* **57**, 2010 (1986).
- [35] D. Hennig, H. Gabriel, G. P. Tsironis, and M. Molina, *Appl. Phys. Lett.* **64**, 2934 (1994).
- [36] Q. Li, C. T. Chan, K. M. Ho, and C. M. Soukoulis, *Phys. Rev. B* **53**, 15577 (1996).
- [37] L. Brillouin and P. Parodi, *Propagation dans les Milieux Périodiques* (Masson-Dunod, Paris, 1956).